Dinuclear (d^3-d^3) Diolate Complexes of Molybdenum and Tungsten. 3.[1] Bridging and Chelating Isomers of $M_2(NMe_2)_2(O{\sim\sim}CHMe{\sim\sim}O)_2$, Where $O{\sim\sim}CHMe{\sim\sim}O$ Is the Dianion of 2,2′-Ethylidenebis(4,6-di-*tert*-butylphenol). Kinetic versus Thermodynamic Considerations

Malcolm H. Chisholm,* Kirsten Folting, William E. Streib, and De-Dong Wu

Department of Chemistry and Molecular Structure Center, Indiana University, Bloomington, Indiana 47405

Received July 7, 1997[⊗]

Hydrocarbon solutions of $Mo_2(NMe_2)_6$ and 2,2′-ethylidenebis(4,6-di-*tert*-butylphenol), $HO{\sim\sim}CHMe{\sim\sim}OH$ (2 equiv), react to give a mixture of two isomers, **A** and **B**, of formula $Mo_2(NMe_2)_2(O{\sim\sim}CHMe{\sim\sim}O)_2$. Both **A** and **B** are shown to contain the bridging μ-$O{\sim\sim}CHMe{\sim\sim}O$ ligands. They are diastereomers differing with respect to the positioning of the CHMe moiety as a result of ring closure with elimination of $HNMe_2$. Compounds **A** and **B** are thermally persistent at 100 °C in the solid state and in toluene, but compound **A** isomerizes in the presence of pyridine to the thermodynamically favored chelate isomer $Mo_2(NMe_2)_2(\eta^2$-$O{\sim\sim}CHMe{\sim\sim}O)_2$, **C**. Compound **C** is related to the previously characterized isomer $Mo_2(NMe_2)_2(\eta^2$-$O{\sim\sim}CH_2{\sim\sim}O)_2$, where the methylene proton that is distal to the Mo−Mo triple bond is replaced by a Me group. Compound **B** cannot rearrange to this isomer without Mo−O bond dissociation. $W_2(NMe_2)_6$ and $HO{\sim\sim}CHMe{\sim\sim}OH$ (2 equiv) react to give $W_2(NMe_2)_2(\eta^2$-$O{\sim\sim}CHMe{\sim\sim}O)_2$, **D**, which is an analogue of **C**. The three molybdenum isomers **A**−**C** and tungsten complex **D** have been structurally characterized by single crystal X-ray studies. The results of this work are discussed in terms of the earlier work involving the related 2,2′-methylenebis(6-*tert*-butyl-4-methylphenoxides) and reveal that the initial ring closure reaction determines the stereochemistry of the subsequent substitution by the biphenoxide at the dinuclear center. Crystal data: for **A**·PhMe at −168 °C, $a = 16.585(5)$ Å, $b = 19.480(6)$ Å, $c = 10.960(3)$ Å, $\alpha = 98.39(2)°$, $\beta = 103.19(1)°$, $\gamma = 91.44(2)°$, space group $P\bar{1}$; for **B**·2PhH at −168 °C, $a = 15.167(3)$ Å, $b = 18.210(3)$ Å, $c = 13.964(3)$ Å, $\alpha = 92.81(1)°$, $\beta = 100.40(1)°$, $\gamma = 71.16(1)°$, space group $P\bar{1}$; for **C**·1.5Et_2O at −168 °C, $a = 16.483(3)$ Å, $b = 16.817(3)$ Å, $c = 14.305(2)$ Å, $\alpha = 106.13(1)°$, $\beta = 108.80(1)°$, $\gamma = 71.70(1)°$, space group $P\bar{1}$; and for **D** at −168 °C, $a = 14.638(2)$ Å, $b = 21.188(4)$ Å, $c = 10.273(2)$ Å, $\alpha = 94.80(1)°$, $\beta = 95.05(1)°$, $\gamma = 100.85(1)°$, space group $P\bar{1}$.

Introduction

Within the field of coordination chemistry the chelate effect has played an influential role in the elucidation of mechanisms of substitutions and rearrangements at mononuclear centers.[2] We have for some time been interested in the development of the coordination chemistry of d^3-d^3 dinuclear complexes of molybdenum and tungsten which show a rich variety of coordination geometries.[3] We have given particular attention to the so-called ethane-like dimers with M−M triple bonds and noted the relatively high barrier to bridge formation in such complexes. Indeed, only one authentic example of the equilibrium shown in eq 1 has been observed thus far.[4]

$$1,2\text{-}W_2(PR_2)_2(NMe_2)_4 \rightleftharpoons W_2(\mu\text{-}PR_2)_2(NMe_2)_4 \qquad (1)$$

As a result of this relatively high barrier it is possible to isolate 1,1- and 1,2-$M_2X_2Y_4$ compounds under kinetic control; *i.e.*, if the thermodynamic isomer is not first formed, the kinetic isomer is persistent even upon heating to *ca.* 100 °C.[5] In reactions between $Mo_2(NMe_2)_6$ and methylenebis(6-*tert*-butyl-4-methylphenol) the bridged isomer $Mo_2(NMe_2)_2(\mu$-$O{\sim\sim}CH_2{\sim\sim}O)_2$ is kinetically formed, and upon addition of pyridine rearrangement to the thermodynamic chelate isomer $Mo_2(NMe_2)_2(\eta^2$-$O{\sim\sim}CH_2{\sim\sim}O)_2$ occurs.[1] A study of the isomerization induced by pyridine (and other Lewis bases) indicated a second order dependence on the concentration of pyridine (py), leading us to propose that two molecules of pyridine were bound in the activated complex which schematically could be represented by eq 2.[1]

$$Mo_2(NMe_2)_2(\mu\text{-}O{\sim\sim}CH_2{\sim\sim}O)_2 + 2Py \rightleftharpoons \left\{ \begin{array}{c} Py \\ N \\ O \\ O \\ Mo \equiv Mo \\ O \\ O \\ N \\ Py \end{array} \right\}^{\ddagger} \rightleftharpoons Mo_2(NMe_2)_2(\eta^2\text{-}O{\sim\sim}CH_2{\sim\sim}O)_2 + 2Py \qquad (2)$$

⊗ Abstract published in *Advance ACS Abstracts,* December 15, 1997.

(1) Part 2: Chisholm, M. H.; Huang, J.-H.; Huffman, J. C.; Parkin, I. P *Inorg. Chem.* **1997**, *36*, 1642.
(2) (a) Basolo, F.; Pearson, R. G. *Mechanisms of Inorganic Reactions. A Study of Metal Complexes in Solution*, 2nd ed.; John Wiley and Sons Publishers: New York, 1968. (b) Wilkins, R. G. *Kinetics and Mechanisms of Transition Metal Complexes*, 2nd ed.; VCH Publishers: Weinheim, Germany, 1991.
(3) Chisholm, M. H. *Acc. Chem. Res.* **1990**, *23*, 419.
(4) Buhro, W. E.; Chisholm, M. H.; Folting, K.; Huffman, J. C.; Martin, J. D.; Streib, W. E. *J. Am. Chem. Soc.* **1988**, *110*, 6563.
(5) Chisholm, M. H.; Folting, K.; Huffman, J. C.; Rothwell, I. P. *Organometallics* **1982**, *1*, 251.

S0020-1669(97)00843-4 CCC: $15.00
Published on Web 01/12/1998

In this work we continue our studies of the substitution of $M_2(NMe_2)_6$ compounds by examining reactions of the closely related 2,2′-ethylidenebis(4,6-di-*tert*-butylphenol), represented for simplicity as HO∼∼CHMe∼∼OH and shown diagramatically as follows.

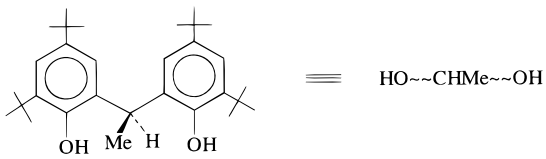

Results and Discussion

Synthesis. Hydrocarbon solutions of $Mo_2(NMe_2)_6$ and 2 equiv of HO∼∼CHMe∼∼OH react to yield orange solutions of $Mo_2(NMe_2)_2(O{\sim\sim}CHMe{\sim\sim}O)_2$. Further replacement of the NMe_2 groups by the biphenol does not occur in the presence of additional HO∼∼CHMe∼∼OH, presumably because of steric crowding at the dimetal center. Also as we have shown previously, as NMe_2 groups are replaced by more electronegative and less π-donating ligands, the M−N σ and π bonds are stabilized and become kinetically less labile toward protonolysis reactions.[6] The kinetically formed solution of $Mo_2(NMe_2)_2(O{\sim\sim}CHMe{\sim\sim}O)_2$ is a mixture of two isomers as is evident by ^{1}H NMR spectroscopy. The two isomers have been separated and purified by taking advantage of their different solubilities in hydrocarbon solvents. Both isomers show, by ^{1}H NMR spectroscopy, four t-Bu singlets in the ratio 1:1:1:1 and two NMe resonances corresponding to proximal and distal Me groups with respect to the Mo≡Mo bond. In one isomer the NMe resonances are notably upfield with respect to the other. In both isomers there is a single C*H* quartet downfield at *ca.* 7 ppm and a single Me doublet. ^{1}H NMR data are given in the Experimental Section. The data are consistent with two isomers each having C_2 symmetry.

The addition of pyridine to a mixture of the two isomers **A** and **B** of formula $Mo_2(NMe_2)_2(\mu\text{-}O{\sim\sim}CHMe{\sim\sim}O)_2$ in hydrocarbon solvents gave upon heating a new compound **C** along with unreacted **B**. As shown in the Experimental Section, we can isolate **A** and **B** in pure forms and thus separately establish that *only* **A** is isomerized to **C** upon heating in the presence of pyridine. Compound **C** showed a more simple ^{1}H NMR spectrum wherein there were two t-Bu singlets of equal intensity, one C*H* and one CH*Me* resonance (a quartet and doublet, respectively) and proximal and distal N*Me* signals. By inference from our earlier work employing the related biphenol HO∼∼CH_2∼∼OH,[1] the isomer **C** could reasonably be formulated as being a chelating isomer $Mo_2(NMe_2)_2(\eta^2\text{-}O{\sim\sim}CHMe{\sim\sim}O)_2$ having either the anti $NO_2Mo\text{-}MoO_2N$ core or one wherein anti ⇌ gauche isomerization was fast on the NMR time scale.

The detailed nature of isomers **A** and **B** could not be inferred from the NMR data, nor was it obvious why only one isomer, isomer **A**, could be transformed to isomer **C**.

We did investigate by ^{1}H NMR spectroscopy the reaction between $Mo_2(NMe_2)_6$ and less than *1 equiv* of HO∼∼CHMe∼∼OH in a J. Young NMR tube. Here we observed, along with the residual $Mo_2(NMe_2)_6$, only one bridging compound that could be reasonably formulated as $Mo_2(NMe_2)_4(\mu\text{-}O{\sim\sim}CHMe{\sim\sim}O)$. With further addition of HO∼∼CHMe∼∼OH this compound was transformed to **A** and **B**. Thus, it was abundantly apparent that the formation of **A** and **B** occurs by separate reaction pathways from a common intermediate, $Mo_2(NMe_2)_4(\mu\text{-}O{\sim\sim}CHMe{\sim\sim}O)$, and that the formation of the second μ-diolate bridge determines the mode of construction of the isomers.

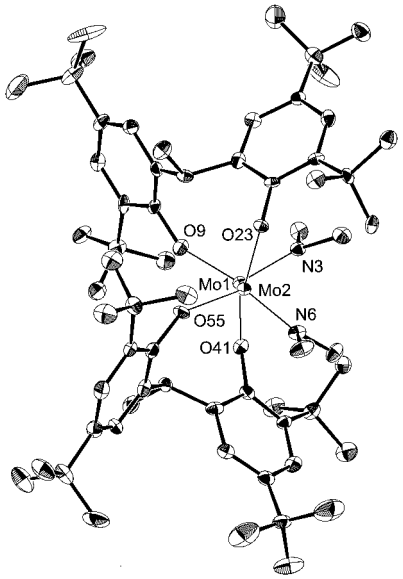

Figure 1. View of the molecular structure (50% thermal ellipsoid probability) of **A** showing the gauche conformation of the central $O_2NMo{\equiv}MoNO_2$ core.

The reaction between $W_2(NMe_2)_6$ and HO∼∼CHMe∼∼OH (2 equiv) under similar conditions gives, quite remarkably, a single product $W_2(NMe_2)_2(\eta^2\text{-}O{\sim\sim}CHMe{\sim\sim}O)_2$ in greater than 60% yield. This is remarkable not only in comparison to the reactions of the related $Mo_2(NMe_2)_6$ described above but because in the reaction involving the related HO∼∼CH_2∼∼OH biphenol C−H activation and oxidative addition to the ditungsten center occurs. This is a reversible process, as shown in eq 3.[1]

The addition of neutral ligands ($HNMe_2$, pyridine) to $W_2(NMe_2)_2(\eta^2\text{-}O{\sim\sim}CHMe{\sim\sim}O)_2$ resulted in no similar C-H activation.

$$W_2(\mu\text{-}H)(NMe_2)_2(\eta^2\text{-}O{\sim\sim}CH_2{\sim\sim}O)(\eta^3\text{-}O{\sim\sim}CH{\sim\sim}O)L \rightleftharpoons W_2(NMe_2)_2(\eta^2\text{-}O{\sim\sim}CH_2{\sim\sim}O)_2 + L \quad (3)$$

Solid State and Molecular Structures. The three isomeric forms of $Mo_2(NMe_2)_2(O{\sim\sim}CHMe{\sim\sim}O)_2$ have been crystallographically characterized. Compounds **A** and **B** contain gauche $O_2NMo-MoNO_2$ cores with virtual (but not crystallographically imposed) C_2 symmetry, as shown in Figures 1 and 2. The bridging μ-O∼∼CHMe∼∼O ligands form nine-membered rings, and in both isomers the phenyl blades are roofed or held in a V shape by the bridging tetrahedral *C*HMe carbon. In both isomers the C*H*Me proton is forced in close proximity to the M≡M bond which accounts for its extreme deshielding, δ 7.00 pm. The Mo to *C*HMe carbon distances in **A** are 3.59 and 3.69 Å and in **B** are 3.42 and 3.84 Å. The C*H*Me protons in **A** are directed toward phenolic oxygen atoms and those in **B** toward the nitrogen atoms of the amide ligands.

Though the conformation of the nine-membered ring is not rigid (except on the NMR time scale), it should be recognized that invertomers of **A** and **B** lead to two different molecules

(6) The PES of $W_2(NMe_2)_2(OR)_4$ compounds reveals the changes in IP's of the NMe_2 lone pairs: Chisholm, M. H.; Tiedtke, D. B.; Gruhn, N. E.; Lichtenbeger, D. L. *Polyhedron*, in press.

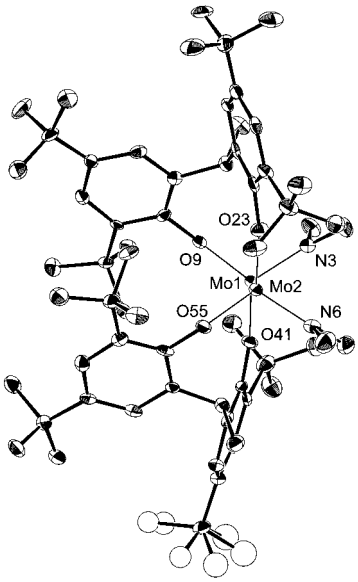

Figure 2. View of the molecular structure (50% thermal ellipsoid probability) of **B** showing the different C*H*Me protons direction from that in **A**. The disorder in one of the *tert*-butyl group methyl carbon atoms is shown.

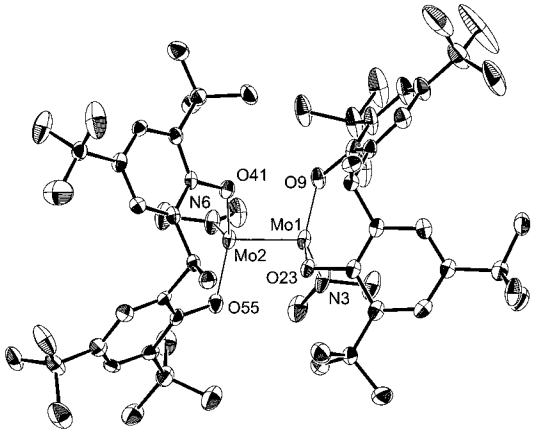

Figure 3. View of the molecular structure (50% thermal ellipsoid probability) of **C** showing the roof shape of the O∼∼CHMe∼∼O ligand directed away from the Mo−Mo bond.

wherein the CH*Me* group would have to be disposed toward the Mo≡Mo center. Molecules **A** and **B** are therefore diastereomers and arise because of the position of the CH*Me* group upon ring closure. In **A** the phenyl groups engulf the NMe_2 ligands which presumably accounts for the upfield shift of the N*Me* signals in the ^{1}H NMR spectra.

The chelate isomer **C** is shown in Figure 3 and is closely related to that seen previously for $Mo_2(NMe_2)_2(\eta^2$-O∼∼CH_2∼∼O$)_2$. It may be viewed as being related by the substitution of the distal ∼CH_pH_d∼ carbon−hydrogen bond by a distal Me group ∼CH_pMe_d∼. Clearly this conformation is favored on steric grounds since a proximal CH*Me* group would cause internal steric congestion.

The tungsten compound **D** does, however, differ from its molybdenum analogue **C** with respect to the disposition of the phenyl blades, as is shown in Figure 4. One phenyl blade in a diolate ligand is nearly parallel to the W≡W bond while the other is nearly perpendicular to it.

Listings of selected bond distances and bond angles for the isomers **A**−**C** and **D** are given in Tables 1 through 4.

Interconversions Involving A−**C**. Careful considerations of the structures of **A** and **B** reveal that they cannot interconvert

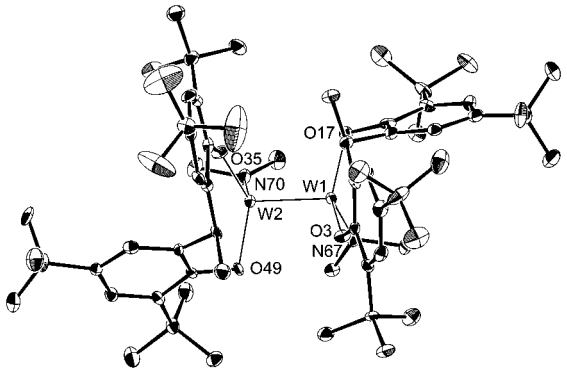

Figure 4. View of the molecular structure (50% thermal ellipsoid probability) of **D** and showing different disposition of the phenyl blades.

Table 1. Selected Distances (Å) and Angles (deg) of Compound **A**

Mo1−Mo2	2.2583(7)	O23−C22	1.365(2)
Mo1−O9	1.925(5)	O41−C42	1.383(5)
Mo1−O41	1.937(3)	O55−C54	1.381(1)
Mo2−O23	1.948(2)	N3−C4	1.466(4)
Mo2−O23	1.948(2)	N3−C5	1.451(6)
Mo2−O55	1.919(3)	N6−C7	1.444(9)
Mo2−N6	1.922(6)	N6−C8	1.454(5)
O9−C10	1.361(7)		
Mo2−Mo1−O9	105.4(1)	O23−Mo2−N6	108.7(1)
Mo2−Mo1−O41	109.6(1)	O55−Mo2−N6	115.4(1)
Mo2−Mo1−N3	103.3(1)	Mo1−O9−C10	153.8(2)
O9−Mo1−O41	113.9(1)	Mo1−O41−C42	133.2(3)
O9−Mo1−N3	115.0(2)	Mo1−N3−C4	114.0(3)
O41−Mo1−N3	109.0(2)	Mo1−N3−C5	134.9(2)
Mo1−Mo2−O23	109.1(1)	Mo2−O23−C22	133.7(2)
Mo1−Mo2−O55	105.1(1)	Mo2−O55−C54	149.6(4)
Mo1−Mo2−N6	103.7(1)	Mo2−N6−C7	134.6(3)
O23−Mo2−N6	108.7(1)	Mo2−N6−C8	113.8(4)

Table 2. Selected Distances (Å) and Angles (deg) of Compound **B**

Mo1−Mo2	2.2486(10)	O23−C22	1.367(9)
Mo1−O9	1.916(5)	O41−C42	1.354(8)
Mo1−O41	1.927(5)	O55−C54	1.376(8)
Mo1−N3	1.926(6)	N3−C4	1.48(1)
Mo2−O23	1.916(5)	N3−C5	1.44(1)
Mo2−O55	1.923(5)	N6−C7	1.46(1)
Mo2−N6	1.919(6)	N6−C8	1.48(1)
O9−C10	1.376(8)		
Mo2−Mo1−O9	110.3(2)	O23−Mo2−N6	115.3(2)
Mo2−Mo1−O41	111.1(2)	O55−Mo2−N6	109.2(2)
Mo2−Mo1−N3	98.8(2)	Mo1−O9−C10	143.6(4)
O9−Mo1−O41	113.9(2)	Mo1−O41−C42	166.6(5)
O9−Mo1−N3	106.5(2)	Mo1−N3−C4	112.5(5)
O41−Mo1−N3	115.2(2)	Mo1−N3−C5	135.4(5)
O41−Mo1−N3	109.9(2)	Mo2−O23−C22	166.8(5)
Mo1−Mo2−Ott	109.0(2)	Mo2−O55−C54	140.7(4)
Mo1−Mo2−N6	99.0(2)	Mo2−N6−C7	135.1(5)
O23−Mo2−O55	113.5(2)	Mo2−N6−C8	115.3(5)

without Mo−O bond dissociation. What was not so immediately obvious to us was why **A** is transformed to **C** in pyridine but **B** is not. However, if we assume that the role of pyridine is one of association, as was seen in the earlier study, then its role is to facilitate terminal to bridge Mo−O bond interconversions. Again, no bonds are actually ever broken in a dissociative sense; merely terminal to bridge to terminal site exchange is promoted by the coordinated pyridine. In this manner isomer **A** can be converted to isomer **C** while **B** cannot. If **B** were to adopt a chelate form related to **C**, then the C*H*Me group would be proximal to the Mo_2 center and this would be sterically disfavored (the Mo to C*H*Me proton distance in **C** is 2.37 Å). However, since the η^2-O∼∼CHMe∼∼O chelate eight-membered ring is not rigid, the central CHMe group could be

Table 3. Selected Distances (Å) and Angles (deg) of Compound **C**

Mo1−Mo2	2.2201(7)	O23−C22	1.374(6)
Mo1−O9	1.944(4)	O41−C42	1.379(6)
Mo1−O23	1.965(3)	O55−C54	1.371(6)
Mo1−N3	1.911(5)	N3−C4	1.462(7)
Mo2−O41	1.943(4)	N3−C5	1.479(8)
Mo2−O55	1.953(4)	N6−C7	1.470(8)
Mo2−N6	1.916(4)	N6−C8	1.467(7)
O9−C10	1.364(7)		
Mo2−Mo1−O9	102.1(1)	O41−Mo2−N6	112.5(2)
Mo2−Mo1−O23	94.3(1)	O55−Mo2−N6	109.9(2)
Mo2−Mo1−N3	106.0(1)	Mo1−O9−C10	132.6(3)
O9−Mo1−O23	129.1(1)	Mo1−O23−C22	102.7(3)
O9−Mo1−N3	109.5(2)	Mo1−N3−C4	115.2(4)
O23−Mo1−N3	111.5(2)	Mo1−N3−C5	133.3(4)
Mo1−Mo2−O41	91.2(1)	Mo2−O41−C42	124.4(3)
Mo1−Mo2−O55	101.4(1)	Mo2−O55−C54	121.4(3)
Mo1−Mo2−N6	106.2(1)	Mo2−N6−C7	135.1(4)
O41−Mo2−O55	130.0(2)	Mo2−N6−C8	114.3(4)

Table 4. Selected Distances (Å) and Angles (deg) of Compound **D**

W1−W2	2.3363(4)	O17−C16	1.377(6)
W1−O3	1.942(1)	O35−C36	1.370(3)
W1−O17	1.964(2)	O49−C48	1.396(6)
W1−N67	1.927(3)	N67−C68	1.471(7)
W2−O35	1.935(2)	N67−C69	1.443(3)
W2−O49	1.964(2)	N70−C71	1.476(7)
W2−N70	1.917(1)	N70−C72	1.468(6)
O3−C4	1.369(1)		
W2−W1−O3	105.6(1)	O35−W2−N70	101.2(1)
W2−W1−O17	101.6(1)	O49−W2−N70	109.5(1)
W2−W12−N67	101.3(1)	W1−O3−C4	136.3(2)
O3−W1−O17	134.2(1)	W1−O17−C16	104.9(2)
O3−W1−N67	101.3(1)	W1−N67−C68	113.3(1)
O17−W1−N67	108.6(1)	W1−N67−C69	134.8(4)
W1−W2−O35	108.9(1)	W2−O35−C36	136.3(1)
W1−W2−O49	101.6(1)	W−O49−C48	103.4(2)
W1−W2−N70	102.8(1)	W2−N70−C71	113.4(2)
O35−W2−O49	130.2(1)	W2−N70−C72	135.2(3)

disposed in an anti manner with respect to the Mo_2 moiety. But, in this conformation the phenyl blades of the biphenoxide are directed inwards (with respect to the Mo_2 center) and now the *t*-Bu groups at each end of the molecule interact in a most unfavorable manner.

What about $W_2(NMe_2)_2(\eta^2\text{-O}\sim\sim\text{CHMe}\sim\sim\text{O})_2$? We are faced with the puzzling situation that the reaction between $W_2(NMe_2)_6$ and 2 equiv of HO∼∼CHMe∼∼OH proceeds directly to one isomer **D**, which is an analogue of **C** described above. How is it that the ditungsten center avoids the bridged analogues **A** and **B** and why does it not undergo C−H activation of the type seen previously? Inspection of the structure of **D** reveals a short W···H−C interaction, as indicated by the W to *C*HMe carbon distance of 2.90 Å. It is always difficult to say why things do not happen and sometimes dangerous to do so because maybe they do but we do not see them. So we merely speculate upon the following.

The W≡W bond is *ca.* 0.08 Å longer than the Mo≡Mo bond in related complexes.[7] It is perhaps just this extra distance that disfavors the second NMe_2 substitution across the bond and favors attack at the *same* metal center. Ring closure would then occur only to give the chelate isomer, and proton NMR spectroscopic data indicate that the reaction between $W_2(NMe_2)_6$ and *ca.* 1 equiv of HO∼∼CHMe∼∼OH forms, in greater than 90% yield, a chelate isomer formulated as $W_2(NMe_2)_4(\eta^2\text{-O}\sim\sim\text{CHMe}\sim\sim\text{O})$. The stereochemistry of the formation of the first ring then determines that of the second to give the sterically favored chelate isomer **D**.

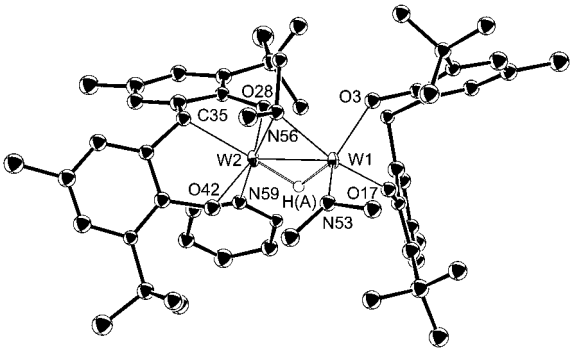

Figure 5. View of the molecular structure (50% thermal ellipsoid probability) of $W_2(H)(NMe_2)_2(\eta^2\text{-O}\sim\sim\text{CH}_2\sim\sim\text{O})(\eta^3\text{-O}\sim\sim\text{CH}\sim\sim\text{O})$-(py) showing the η^3-O∼∼CH∼∼O ligand bond to W_2.

It could, however, be that $W_2(NMe_2)_6$ reacts with HO∼∼CHMe∼∼OH to give a kinetically labile product $W_2(H)$-$(NMe_2)_2(\eta^2\text{-O}\sim\sim\text{CHMe}\sim\sim\text{O})(\eta^3\text{-O}\sim\sim\text{CMe}\sim\sim\text{O})(HNMe_2)$ which then converts to $W_2(NMe_2)_2(\eta^2\text{-O}\sim\sim\text{CHMe}\sim\sim\text{O})_2$. Possible evidence for this notion comes from the observation that the crude reaction mixture containing the products from the reaction between $W_2(NMe_2)_6$ and 2 equiv of HO∼∼CHMe∼∼OH obtained from removal of the solvent under a dynamic vacuum is a brown foamy substance which shows a complicated ^{1}H NMR spectrum. However, recrystallization from hydrocarbon solvents yields a clean orange crystalline product $W_2(NMe_2)_2(\eta^2\text{-O}\sim\sim\text{CHMe}\sim\sim\text{O})_2$. In toluene-$d_8$ this product shows no reactivity toward added pyridine-d_5 of the type shown in eq 3.[1] Given the close proximity of the ∼C*H*Me hydrogen atom to the W_2^{6+} center, one must surely wonder why C−H activation does not occur in this compound. A possible clue to this may be found in the structure of the complex W_2-$(H)(NMe_2)_2(\eta^2\text{-O}\sim\sim\text{CH}_2\sim\sim\text{O})(\eta^3\text{-O}\sim\sim\text{CH}\sim\sim\text{O})$(py) shown in Figure 5. (The distance between N56 and the hydrogen related to C35 is 2.67 Å). If the product of CH activation, W_2-$(H)(NMe_2)_2(\eta^2\text{-O}\sim\sim\text{CHMe}\sim\sim\text{O})(\eta^3\text{-O}\sim\sim\text{CMe}\sim\sim\text{O})$(py), had a related structure, the position of the methyl group of the metallated η^3-O∼∼CMe∼∼O ligand would cause unfavorable internal steric congestion. Thus, an equilibrium of the type shown in eq 3 might occur but merely lie in favor of $W_2(NMe_2)_2$-$(\eta^2\text{-O}\sim\sim\text{CHMe}\sim\sim\text{O})_2$. The stereochemical consequences of CH activation with respect to bridged isomers of types **A** and **B** are not known. Further speculation is not profitable.

Concluding Remarks

The reactions between $Mo_2(NM_2)_6$ and HO∼∼CHMe∼∼OH (2 equiv) reveal that the initial mode of chelation of the diolate, or ring closure with elimination of $HNMe_2$, occurs across the Mo−Mo bond. The second substitution and ring closure can occur in one of two ways so that two isomers **A** and **B** are formed competitively. Isomerization is not possible without Mo−O bond cleavage, and this does not take place below 100 °C. It is interesting to note that an isomer having a mixed arrangement of the μ-diolate ligands is not observed.

The addition of pyridine allows the isomerizaton of only **A** to the chelate isomer **C**, which is with respect to **A** the thermodynamic isomer. Isomer **B** cannot rearrange to **C** without Mo−O bond cleavage, and a chelate form derived from **B** is presumably not favored because of steric factors.

The reaction of $W_2(NMe_2)_6$ with the HO∼∼CHMe∼∼OH biphenol (2 equiv) to give only the chelate isomer **D** is quite

(7) Cotton, F. A.; Walton, R. A. *Multiple Bonds between Metal Atoms*, 2nd Ed.; Oxford University Press: Oxford, U.K., 1993.

Table 5. Summary of Crystal Data

	A·PhMe	**B**·2PhH	**C**·1.5Et$_2$O	**D**
chem formula	$C_{71}H_{108}Mo_2N_2O_4$	$C_{76}H_{112}Mo_2N_2O_4$	$C_{70}H_{115}Mo_2N_2O_{5.5}$	$C_{64}H_{100}N_2O_4W_2$
fw	1245.53	1309.62	1264.58	1329.19
space group	$P\bar{1}$	$P\bar{1}$	$P\bar{1}$	$P\bar{1}$
T (°C)	−168	−168	−168	−168
a (Å)	16.585(5)	15.167(3)	16.483(3)	14.638(2)
b (Å)	19.480(6)	18.210(3)	16.817(3)	21.188(4)
c (Å)	10.960(3)	13.964(3)	14.305(2)	10.273(2)
α (deg)	98.39(2)	92.81(1)	106.13(1)	94.80(1)
β (deg)	103.19(1)	100.40(1)	108.80(1)	95.05(1)
γ (deg)	91.44(2)	71.16(1)	71.70(1)	100.85(1)
V (Å^3)	3404.30	3590.11	3494.14	3100.75
Z	2	2	2	2
ρ_{calcd} (g cm^{-3})	1.215	1.211	1.202	1.424
wavelength λ (Å)	0.710 69	0.710 69	0.710 69	0.710 69
μ (cm^{-1})	4.137	3.957	4.055	37.563
$R(F)^a$	0.0579	0.0589	0.0503	0.0280
$R_w(F)^b$	0.0554	0.0556	0.0553	0.0325

^{a} $R = \sum||F_o| - |F_c||/\sum|F_o|$. ^{b} $R_w = \{\sum w(|F_o| - |F_c|)^2/\sum wF_o^2\}^{1/2}$, where $w = 1/[\sigma^2(|F_o|)]$.

remarkable. It is possible that subtle differences in the substitution reaction pathways of the $Mo_2(NMe_2)_6$ and $W_2(NMe_2)_6$ may allow for the direct formation of the chelate complex $W_2(NMe_2)_2(\eta^2$-O∼∼CHMe∼∼O)$_2$, **D**, an analogue of **C**, without the formation of kinetic bridged (μ-O∼∼CHMe∼∼O) containing compounds. Alternatively a reversible C*H*Me metallation reaction may lead to ligand isomerization via an (η^3-O∼∼CMe∼∼O) complex (or complexes) which is (are) unstable with respect to the $W_2(NMe_2)_2(\eta^2$-O∼∼CHMe∼∼O)$_2$ complex because of steric factors. It does not seem to be possible to distinguish between the latter possibilities at this time.

The present work emphasizes how the use of chelating ligands at dimetal centers may allow insight into detailed reaction pathways of substitution chemistry. It is also interesting to note that in substitution reactions at Mo_2^{4+} centers with M−M quadruple bonds chelating isomers are often kinetically formed and then transformed to the thermodynamic bridged isomers when the entering ligands are ethylene linked -diphosphines or -diarsines.[7] The mechanisms of their interconversions have been discussed in terms of an internal flip rearrangement, [8] which is in effect related to the non-dissociative isomerizations described herein.

Experimental Section

All reaction manipulations were carried out in a glovebox or Schlenk line under a nitrogen atmosphere. Solvents were dried by distillation over sodium dispersion/benzophenone under a nitrogen atmosphere. ^{1}H and ^{13}C{^{1}H} NMR spectra were recorded on a Varian XL-300 NMR spectrometer and referenced to the residual protio impurities of the deuterated benzene. $M_2(NMe_2)_6$ compounds were prepared as described elsewhere.[9] 2,2′-Ethylidenebis(4,6-di-*tert*-butylphenol) was purchased from Aldrich Chemical Co., Inc.

$Mo_2(NMe_2)_2(\mu$-O∼∼CHMe∼∼O)$_2$, A. A 100 mL Schlenk flask was charged with $Mo_2(NMe_2)_6$ (456 mg, 1.0 mmol) and biphenol (880 mg, 2.0 mmol). To the mixture was added 30 mL of toluene. After the resultant solution was stirred overnight, pure **A** was deposited as a yellow precipitate, which was collected by filtration and dried under vacuum (yield: 31%, 363 mg). Orange crystals of **A**·PhMe suitable for X-ray analysis were obtained by slowly cooling the toluene solution. ^{1}H NMR data (C_6D_6): δ 7.87 (d, aromatic protons, 2H, J_{H-H} = 2.4 Hz), 7.54 (d, aromatic protons, 4H, J_{H-H} = 2.4 Hz), 7.39 (d, aromatic protons, 2H, J_{H-H} = 2.4 Hz), 7.16 (q, C*H*Me, 2H, J_{H-H} = 6.9 Hz), 3.87 (s, N*Me*, 6H), 2.58 (s, N*Me*,6H), 1.73 (d, CH*Me*, 6H, J_{H-H} = 2.4 Hz), 1.55 (s, C*Me*$_3$, 18H), 1.48 (s, C*Me*$_3$, 18H), 1.37 (s, C*Me*$_3$, 18H), 1.26 (s, C*Me*$_3$, 18H). ^{13}C NMR data (C_6D_6): δ 165.0, 159.5, 143.9, 142.5, 138.4, 138.3, 136.9, 132.4, 124.6, 122.0, 121.7, 121.0 (phenyl carbon), 60.2 (N*Me*), 43.5 (*C*HMe), 36.5 (*C*Me$_3$), 35.7 (*C*Me$_3$), 35.3 (*C*Me$_3$), 34.9 (N*Me*), 32.4 (C*Me*$_3$), 31.3 (C*Me*$_3$), 31.1 (C*Me*$_3$), 27.0 (CH*Me*). Anal. Calcd for $C_{64}H_{100}N_2O_4Mo_2$·C_7H_8: C, 68.47; H, 8.74; N, 2.43. Found: C, 68.32; H, 8.66; N, 2.33.

$Mo_2(NMe_2)_2(\mu$-O∼∼CHMe∼∼O)$_2$, B. The above filtrate was stripped under a dynamic vacuum, and the residue was washed with 10 mL of hexane in two portions and then dried in vacuum. A mixture of **A** and **B** at a ratio of *ca*. 1:4 was isolated (**A** and **B** total yield: 65%, 386 mg). 110 mg amount of mixture was suspended in 6 mL of pyridine, and the mixture was gently refluxed for 20 min. After cooling, the solvent was removed under a dynamic vacuum. The residue was washed with 8 mL of hexane and then dried under vacuum to give a yellow powder of pure **B** (76 mg). Orange crystals of **B**·2PhH suitable for X-ray analysis were obtained by slowly cooling the benzene solution. ^{1}H NMR data (C_6D_6): δ 7.97 (d, aromatic protons, 2H, J_{H-H} = 2.1 Hz), 7.56 (d, aromatic protons, 2H, J_{H-H} = 2.1 Hz), 7.50 (d, aromatic protons, 2H, J_{H-H} = 2.1 Hz), 7.31 (d, aromatic protons, 2H, J_{H-H} = 2.1 Hz), 6.99 (q, C*H*Me, 2H, J_{H-H} = 7.2 Hz), 4.30 (s, N*Me*, 6H), 2.98 (s, N*Me*,6H), 1.68 (d, CH*Me*, 6H, J_{H-H} = 7.2 Hz), 1.58 (s, C*Me*$_3$, 18H), 1.39 (s, C*Me*$_3$, 18H), 1.32 (s, C*Me*$_3$, 18H), 1.03 (s, C*Me*$_3$, 18H). ^{13}C-{^{1}H} NMR data (C_6D_6): δ 162.6, 158.1, 143.7, 142.7, 137.8, 137.7, 135.5, 134.7, 124.1, 122.5, 121.5 (phenyl carbon), 58.5 (N*Me*), 46.6 (*C*HMe), 35.9 (*C*Me$_3$), 35.8 (*C*Me$_3$), 35.3 (*C*Me$_3$), 32.5 (C*Me*$_3$), 32.3 (C*Me*$_3$), 30.9 (C*Me*$_3$), 30.5 (N*Me*), 30.2 (C*Me*$_3$), 24.6 (CH*Me*). Anal. Calcd for $C_{64}H_{100}N_2O_4Mo_2$·C_6H_6: C, 68.27; H, 8.67; N, 2.27. Found: C, 67.95; H, 8.86; N, 2.34.

$Mo_2(NMe_2)_2(\eta^2$-O∼∼CHMe∼∼O)$_2$, C. Pure **A** (105 mg, 0.09 mmol) in 8 mL of pyridine was gently refluxed for 20 min, and the solvents were removed under a dynamic vacuum to yield a brown powder of pure **C** (yield: 90%, 94 mg). Amber crystals of **C**·1.5Et$_2$O suitable for X-ray analysis were obtained from slow evaporation of the ether solution. ^{1}H NMR data (C_6D_6): δ 7.67 (d, aromatic protons, 4H, J_{H-H} = 2.4 Hz), 7.46 (d, aromatic protons, 4H, J_{H-H} = 2.4 Hz), 5.90 (q, C*H*Me, 2H, J_{H-H} = 6.3 Hz), 4.37 (s, N*Me*, 6H), 1.73 (d, CH*Me*, 6H, J_{H-H} = 6.3 Hz), 1.72 (s, C*Me*$_3$, 36H), 1.49 (s, N*Me*, 6H), 1.34 (s, C*Me*$_3$, 36H). ^{13}C{^{1}H} NMR data (C_6D_6): δ 154.8, 143.4, 139.7, 134.8, 123.0, 122.4 (phenyl carbon), 59.0 (N*Me*), 39.9 (*C*HMe), 36.4 (*C*Me$_3$), 35.0 (*C*Me$_3$), 32.5 (N*Me*), 32.2 (C*Me*$_3$), 30.6 (C*Me*$_3$), 26.9 (CH*Me*). Anal. Calcd for $C_{64}H_{100}N_2O_4Mo_2$: C, 66.67; H, 8.74; N, 2.43. Found: C, 67.01; H, 8.84; N, 2.20.

$W_2(NMe_2)_2(\eta^2$-O∼∼CHMe∼∼O)$_2$, D. A 30 mL Schlenk flask was charged with $W_2(NMe_2)_6$ (320 mg, 0.5 mmol) and biphenol (441 mg,

(8) (a) Cotton, F. A.; Kitagawa, S. *Polyhedron* **1988**, *7*, 463. (b) McVilie, A.; Peacock, R. D. *Polyhedron* **1992**, *11*, 2531. (c) Agaskar, P. A.; Cotton, F. A. *Inorg. Chem.* **1986**, *25*, 15. (d) Cayton, R. H.; Chisholm, M. H. *Inorg. Chem.* **1991**, *30*, 1422.

(9) (a) M = Mo: Chisholm, M. H.; Haitko, D. A.; Murrillo, C. A. *Inorg. Synth.* **1982**, *21*, 5. (b) M = W: Chisholm, M. H.; Martin, J. D. *Inorg. Synth.* **1992**, *29*, 137.

1.0 mmol). To the mixture was added 10 mL of toluene. After the resultant solution was stirred for 6 h, then the volatile components were removed under a dynamic vacuum to give a foamy solid, which was dissolved in 5 mL of hexane. Pure **D** was obtained as a brown microcrystalline solid (yield: 66%, 440 mg). Orange crystals of **D** suitable for X-ray analysis were obtained by slow evaporation of the hexane solution. ^{1}H NMR data (C_6D_6): δ 7.63 (d, aromatic protons, 4H, J_{H-H} = 2.4 Hz), 7.49 (d, aromatic protons, 4H, J_{H-H} = 2.4 Hz), 5.26 (q, C*H*Me, 2H, J_{H-H} = 6.3 Hz), 4.43 (s, N*Me*, 6H), 1.71 (s, C*Me*$_3$, 36H), 1.66 (d, CH*Me*, 6H, J_{H-H} = 6.3 Hz), 1.54 (s, N*Me*, 6H), 1.33 (s, C*Me*$_3$, 36H). ^{13}C{^{1}H} NMR data (C_6D_6); δ153.1, 143.7, 139.9, 134.1, 122.8 (phenyl carbon), 60.6 (N*Me*), 37.1 (*C*HMe), 36.4 (*C*Me$_3$), 35.0 (*C*Me$_3$), 33.0 (N*Me*), 32.2 (C*Me*$_3$), 30.6 (C*Me*$_3$), 26.6 (CH*Me*). Anal. Calcd for $C_{64}H_{100}N_2O_4W_2$: C, 57.83; H, 7.58; N, 2.11. Found: C, 58.12; H, 7.69; N, 1.92.

Selected 1H NMR data, as determined by an NMR tube reaction (C_6D_6): for $Mo_2(NMe_2)_4(\mu$-O∼∼CHMe∼∼O), δ 7.91 (d, aromatic protons, 1H, J_{H-H} = 2.4 Hz), 7.58 (d, aromatic protons, 1H, J_{H-H} = 2.4 Hz), 7.51 (d, aromatic protons, 1H, J_{H-H} = 2.4 Hz), 7.46 (d, aromatic protons, 1H, J_{H-H} = 2.4 Hz), 7.07 (q, C*H*Me, 1H, J_{H-H} = 7.2 Hz), 1.71 (d, CH*Me*, 3H, J_{H-H} = 2.4 Hz), 1.70 (s, C*Me*$_3$, 9H), 1.58 (s, C*Me*$_3$, 9H), 1.36 (s, C*Me*$_3$, 9H), 1.29 (s, C*Me*$_3$, 9H); for $W_2(NMe_2)_4$-(η^2-O∼∼CHMe∼∼O), 7.50 (d, aromatic protons, 2H, J_{H-H} = 2.4 Hz), 7.37 (d, aromatic protons, 2H, J_{H-H} = 2.4 Hz), 4.69 (q, C*H*Me, 2H, J_{H-H} = 7.2 Hz), 1.70 (d, CH*Me*, 6H),1.53 (s, C*Me*$_3$, 18H), 1.34 (s, C*Me*$_3$, 18H).

Crystallographic Studies. General operating procedures and a listing of programs have been given previously.[10] A summary of crystal data is given in Table 5.

Full details of the four structural determination are available via the Internet as indicated in the Supporting Information.

Acknowledgment. We thank the National Science Foundation for financial support.

Supporting Information Available: Tables giving a summary of data collection, atomic coordinates, and complete listings of bond distances and angles for A−D (41 pages). Ordering information is given on any current masthead page. The complete structural reports are available from the reciprocal data base via Internet at url http://www.iumsc.indiana.edu. For **A**·PhMe request Report No. 97036; for **B**·2PhH, Report No. 97043; for **C**·1.5Et$_2$O, Report No. 97048; and for **D**, Report No. 96210.

IC9708430

(10) Chisholm, M. H.; Folting, K.; Huffman, J. C.; Kirkpatrick, C. C. *Inorg. Chem.* **1984**, *23*, 1021.